

Evidence for Mixed Mg Coordination Environments in Silicate Glasses: Results from ^{25}Mg NMR Spectroscopy at 35.2 T

Sabyasachi Sen,* Jonathan F. Stebbins, Scott Kroeker, Ivan Hung, and Zhehong Gan



Cite This: *J. Phys. Chem. B* 2023, 127, 10659–10666



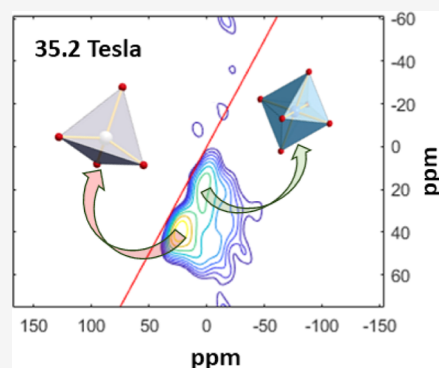
Read Online

ACCESS |

Metrics & More

Article Recommendations

ABSTRACT: The Mg–O coordination environment of silicate glasses of composition $\text{CaMgSi}_2\text{O}_6$, $\text{Na}_2\text{MgSi}_3\text{O}_8$, and $\text{K}_2\text{MgSi}_5\text{O}_{12}$ is probed using ultrahigh-field (35.2 T) ^{25}Mg magic angle spinning nuclear magnetic resonance (MAS NMR) and triple-quantum MAS NMR spectroscopy. These spectra clearly reveal the coexistence of 4-fold- (Mg^{IV}) and 6-fold- (Mg^{VI}) coordinated Mg in all glasses. The $\text{Mg}^{\text{IV}}/\text{Mg}^{\text{VI}}$ ratio implies an average Mg–O coordination number of ~ 5 for $\text{CaMgSi}_2\text{O}_6$ glass, bringing NMR results for the first time in good agreement with those reported in previous studies based on diffraction and X-ray absorption spectroscopy, thus resolving a decade-long controversy regarding Mg coordination in alkaline-earth silicate glasses. The Mg–O coordination number decreases to ~ 4.5 in the alkali–Mg silicate glasses, indicating that Mg competes effectively with the low field strength alkali cations for the nonbridging oxygen in the structure to attain tetrahedral coordination. This work illustrates the promise of ultrahigh-field NMR spectroscopy in structural studies involving nuclides with low gyromagnetic ratio.



1. INTRODUCTION

Recent studies have indicated that Mg plays a key role as a constituent element in silicate glasses in improving their crack and corrosion resistance as well as certain aspects of their bioactivity.^{1,2} Moreover, Mg is an important geochemical constituent in many natural silicate melts or magmas that exerts significant control on the transport properties and mineral–melt equilibria.^{3–5} These functional roles of Mg are critically dependent on its bonding and coordination environment in the structures of silicate glasses and liquids. On one hand, it is well-established that the addition of MgO to a silicate glass results in the formation of nonbridging oxygen atoms (NBOs). In that sense, it can be argued that MgO plays the role of a modifier oxide.⁶ On the other hand, increasing addition of MgO to SiO_2 beyond 50 mol % results in an increase in the glass transition temperature, which could be suggestive of the participation of strong Mg–O bonds in the integrity of the structural network.⁷

However, despite a large number of structural studies utilizing a variety of spectroscopic and diffraction methods, the nature of the Mg–O coordination environment in silicate glasses has remained rather controversial in the literature. For example, previous X-ray absorption spectroscopic studies at the Mg K-edge indicated the presence of Mg^{IV} (tetrahedral or 4-fold coordination), Mg^{V} (5-fold coordination), and Mg^{VI} (octahedral or 6-fold coordination) environments in the structure of $\text{CaMgSi}_2\text{O}_6$ glass.^{8,9} On the other hand, ^{25}Mg magic angle spinning nuclear magnetic resonance (MAS NMR) studies conducted at a magnetic field of 14.1 T by

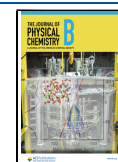
Kroeker and Stebbins indicated that, like crystalline $\text{CaMgSi}_2\text{O}_6$, Mg is present predominantly as Mg^{VI} in the structure of the glass of the same composition.¹⁰ The same conclusion was reached by Sen et al. for glasses along the join $\text{Mg}_2\text{SiO}_4\text{–MgSiO}_3$ based on ^{25}Mg MAS NMR spectra acquired at a magnetic field of 21.8 T and by Shimoda et al. for MgSiO_3 , $\text{CaMgSi}_2\text{O}_6$, and a few other Ca, Mg silicate and aluminosilicate glasses on the basis of ^{25}Mg triple-quantum MAS (3QMAS) NMR studies at 16.4 and 21.8 T.^{6,11,12} These results on the Mg coordination environment in MgSiO_3 and $\text{CaMgSi}_2\text{O}_6$ glasses have recently been corroborated in a ^{25}Mg NMR study conducted at 14.1 T by Eckert and co-workers;¹³ but this study also indicated that the presence of multiple Mg coordination environments in these glasses cannot be precluded solely on the basis of NMR data at these moderate magnetic fields. In contrast, isotope-substituted neutron diffraction studies by Cormier and Cuello and combined X-ray and neutron diffraction and reverse Monte Carlo simulation by Wilding et al. indicated that Mg is present predominantly as Mg^{IV} in MgSiO_3 and other MgO–SiO_2

Received: September 25, 2023

Revised: November 1, 2023

Accepted: November 8, 2023

Published: November 30, 2023



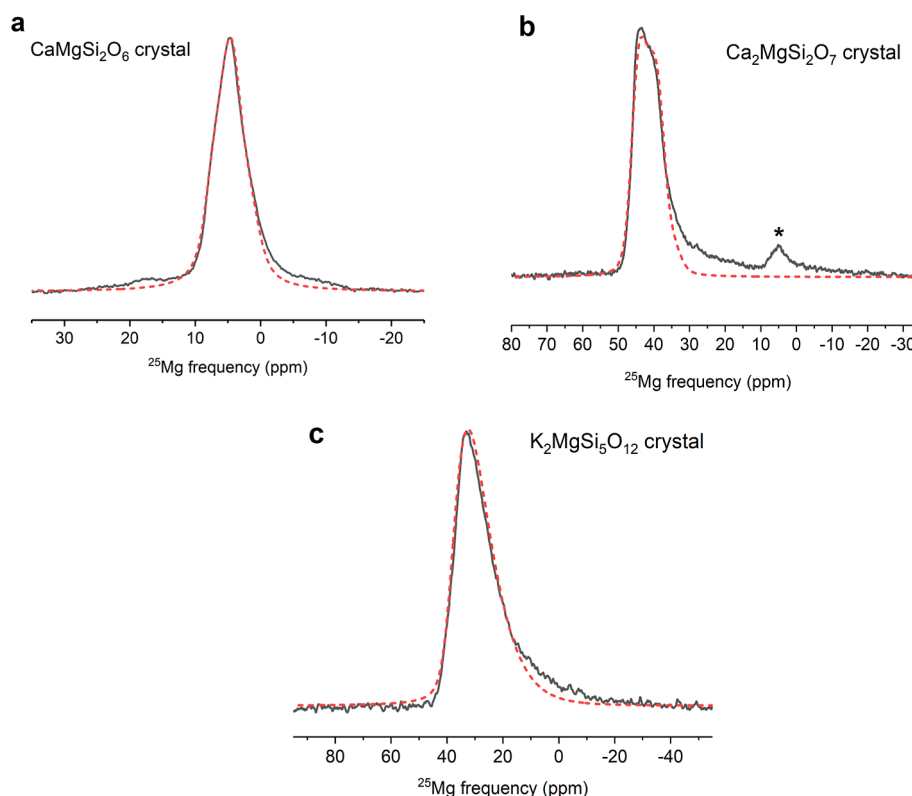


Figure 1. Experimental (solid black line) and simulated (dashed red line) ultrahigh-field (35.2 T) ^{25}Mg MAS NMR spectra of crystalline silicates: (a) $\text{CaMgSi}_2\text{O}_6$, (b) $\text{Ca}_2\text{MgSi}_2\text{O}_7$, and (c) $\text{K}_2\text{MgSi}_5\text{O}_{12}$. Resonance marked by an asterisk in (b) corresponds to the $\text{CaMgSi}_2\text{O}_6$ secondary phase. Simulation parameters are listed in Table 1.

glasses, with an average Mg–O coordination number ranging between 4.4 and 4.8.^{7,14,15}

Such a significant discrepancy between diffraction and NMR results may be indicative of the challenges associated with each technique for the determination of the coordination environment of cations, such as Mg. While, for diffraction, a distorted nearest-neighbor environment may lead to an erroneous estimation of the coordination number of an atom, NMR spectroscopy of the ^{25}Mg nuclide presents its own formidable challenges owing to the low gyromagnetic ratio of this nuclide, combined with its low natural abundance (10%) and large quadrupolar broadening. These challenges with ^{25}Mg NMR can be circumvented by isotopically enriching the samples with ^{25}Mg and by performing MAS and multiple-quantum MAS (MQMAS) NMR spectroscopy at ultrahigh magnetic fields (>20 T) to minimize or eliminate the effects of quadrupolar broadening. The MQMAS experiment is a two-dimensional NMR spectroscopic technique that averages out the second-order line-broadening effects from quadrupolar interactions for $I > 1/2$ nuclides such as ^{25}Mg ($I = 5/2$), by mixing single- and multiple-quantum coherences to generate a high-resolution isotropic spectrum in one dimension, which is correlated in the second dimension with the single-quantum MAS central-transition spectrum.¹⁶ The isotropic spectrum is only broadened by the distributions of the chemical shift and the isotropic quadrupolar shift. Here we present high-resolution ^{25}Mg MAS and 3QMAS NMR spectroscopic data on select crystalline and glassy alkali and alkaline-earth Mg silicates obtained at an ultrahigh magnetic field of 35.2 T. These spectra reveal the Mg coordination environment in these materials to unprecedented accuracy and conclusively demon-

strate the coexistence of multiple Mg–O coordination environments in silicate glasses, which resolves the above-mentioned inconsistency between the NMR and the diffraction results reported in previous studies in the literature.

2. MATERIALS AND METHODS

2.1. Materials. The crystalline $\text{CaMgSi}_2\text{O}_6$ (diopside), $\text{Ca}_2\text{MgSi}_2\text{O}_7$ (akermanite), and $\text{K}_2\text{MgSi}_5\text{O}_{12}$ and glassy $\text{CaMgSi}_2\text{O}_6$, $\text{Na}_2\text{MgSi}_3\text{O}_8$, and $\text{K}_2\text{MgSi}_5\text{O}_{12}$ samples used in this study are the same ones used in a previous ^{25}Mg NMR study by Kroeker and Stebbins,¹⁰ except the glass samples were all rejuvenated for this study before the NMR data collection by melting them at 1450 °C for 1 h in a platinum crucible followed by quenching in air. All samples were originally prepared by Kroeker and Stebbins using 96.75% ^{25}Mg -enriched MgO .¹⁰ The crystalline compounds were prepared via solid-state synthesis, and their phase identification was carried out using powder X-ray diffraction. The glasses were prepared by using the typical melt-quenching route. Details of the sample synthesis can be found in that study.

2.2. Ultrahigh-Field ^{25}Mg NMR. ^{25}Mg solid-state NMR experiments recorded at 35.2 T were performed on the series-connected hybrid (SCH) magnet (^{25}Mg Larmor frequency of 91.83 MHz) at the National High Magnetic Field Laboratory (NHMFL) in Tallahassee, USA.¹⁷ A Bruker AVANCE NEO console and a single-resonance MAS probe designed and constructed at the NHMFL were used with 3.2 mm o.d. pencil-style rotors spinning at a MAS frequency of 17.86 kHz. The 1D NMR spectra for the crystalline $\text{CaMgSi}_2\text{O}_6$ (diopside), $\text{Ca}_2\text{MgSi}_2\text{O}_7$ (akermanite), and $\text{K}_2\text{MgSi}_5\text{O}_{12}$ samples were obtained using a single-pulse direct excitation of 2 μs , r_f field of

14.9 kHz, recycle delay of 1 s, and 1024 averaged transients. For the $\text{CaMgSi}_2\text{O}_6$, $\text{K}_2\text{MgSi}_5\text{O}_{12}$, and $\text{Na}_2\text{MgSi}_3\text{O}_8$ glass samples, the 1D NMR spectra were acquired using QCPMG¹⁸ signal enhancement with $\pi/2$ and π pulses of 3 and 6 μs , 0.5 s recycle delay, 54 CPMG pulse acquisition loops with each loop lasting 20 rotor periods, and 3840, 5120, and 8192 averaged transients, respectively. A phase-modulated split- t_1 shifted-echo sequence¹⁹ was used for acquisition of the 2D 3QMAS NMR spectra in combination with QCPMG for signal enhancement. Pulses of 9.9 and 3.3 μs with rf field of ~ 44 kHz were used for 3Q excitation and conversion, along with soft pulses of 5 and 10 μs at 16.7 kHz rf field, 0.5 s recycle delay, and 68 CPMG pulse-acquisition loops, with each loop lasting 20 rotor periods. Acquisition of the t_1 evolution was performed by rotor synchronization of the delay between the 3Q excitation and conversion pulses; 8 complex t_1 points were acquired for each spectrum with a total of 2880, 8640, and 5760 and averaged transients per t_1 point for the $\text{CaMgSi}_2\text{O}_6$, $\text{K}_2\text{MgSi}_5\text{O}_{12}$, and $\text{Na}_2\text{MgSi}_3\text{O}_8$ glass samples, respectively. ^{25}Mg NMR spectra were externally referenced by recording the ^{17}O signal of D_2O and using the ^{17}O and ^{25}Mg frequency ratios reported in the IUPAC recommendations.²⁰

3. RESULTS AND DISCUSSION

The ultrahigh-field ^{25}Mg MAS NMR spectra of the three crystalline compounds $\text{CaMgSi}_2\text{O}_6$ (diopside), $\text{Ca}_2\text{MgSi}_2\text{O}_7$ (akermanite), and $\text{K}_2\text{MgSi}_5\text{O}_{12}$ are shown in Figure 1. The center bands of these central-transition line shapes were simulated using the ssNake software package to obtain the NMR parameters including the isotropic chemical shift δ_{iso} , the quadrupolar coupling constant C_Q , and the asymmetry parameter η of the electric field gradient tensor at the site of the nucleus.²¹ As shown in Table 1, the resulting NMR

Table 1. ^{25}Mg NMR Parameters for Crystalline Compounds Obtained from Simulation of Spectra Acquired at 35.2 T^a

composition	δ_{iso} (± 0.5 ppm)	C_Q (± 0.1 MHz)	η (± 0.05)
$\text{Ca}_2\text{MgSi}_2\text{O}_7$ (akermanite)	47.4 (47.0)	2.9 (2.8)	0.23 (0.20)
$\text{CaMgSi}_2\text{O}_6$ (diopside)	8.4 (8.0)	2.1 (2.1)	0.75 (0.75)
$\text{K}_2\text{MgSi}_5\text{O}_{12}$	39.2 (30–50)	3.1 (<3.7)	0.00

^aValues in parentheses are from ref 10.

parameters are consistent with those obtained in a previous study by Kroeker and Stebbins from simulation of low-field (14.1 T) line shapes on the same samples.¹⁰ It is apparent from Figure 1 that while the central-transition MAS line shapes of crystalline $\text{CaMgSi}_2\text{O}_6$ and $\text{Ca}_2\text{MgSi}_2\text{O}_7$ can be described well with a single set of δ_{iso} , C_Q , and η , that of crystalline $\text{K}_2\text{MgSi}_5\text{O}_{12}$ requires a distribution of quadrupolar parameters. This difference was explained by Kroeker and Stebbins¹⁰ to be due to a disordered structure of the $\text{K}_2\text{MgSi}_5\text{O}_{12}$ sample, owing to its synthesis conditions. An extended Cjzek distribution of the quadrupolar parameters^{21,22} was therefore employed within the ssNake program to simulate the ^{25}Mg NMR line shape for this crystal. The Mg atoms are known to be octahedrally coordinated in crystalline $\text{CaMgSi}_2\text{O}_6$, and tetrahedrally coordinated in $\text{K}_2\text{MgSi}_5\text{O}_{12}$ and $\text{Ca}_2\text{MgSi}_2\text{O}_7$, consistent with their ^{25}Mg NMR δ_{iso} values of ~ 8 , 39, and 47 ppm, respectively, as obtained from these simulations (Table 1). It may be noted here that in the present study, the significant lowering of the quadrupolar broadening in the ultrahigh-field

^{25}Mg MAS NMR spectra of these crystals reveals the presence of a small amount ($\sim 4\%$) of a secondary “impurity” phase in the $\text{Ca}_2\text{MgSi}_2\text{O}_7$ sample in the form of a resonance centered near ~ 5 ppm (Figure 1). The presence of this phase went undetected in the lower-field ^{25}Mg MAS NMR spectrum of this sample in the previous study by Kroeker and Stebbins.¹⁰ Moreover, the small fraction of this phase must have remained undetected in their powder X-ray diffraction measurement as well. The spectral line shape of this resonance could indeed be simulated with a set of NMR δ_{iso} , C_Q , and η that is consistent with this secondary phase being crystalline $\text{CaMgSi}_2\text{O}_6$.

The ultrahigh-field ^{25}Mg MAS NMR spectra of the three glasses ($\text{CaMgSi}_2\text{O}_6$, $\text{K}_2\text{MgSi}_5\text{O}_{12}$, and $\text{Na}_2\text{MgSi}_3\text{O}_8$) investigated in this study are shown in Figure 2. These spectral line shapes can be simulated well, with a single site having an extended Cjzek distribution of quadrupolar parameters (Table 2). A direct comparison between the ^{25}Mg NMR parameters (Tables 1 and 2) of the crystalline and glassy phases of $\text{CaMgSi}_2\text{O}_6$ and $\text{K}_2\text{MgSi}_5\text{O}_{12}$ shows relatively small change in δ_{iso} between the crystal and the glass, suggesting that Mg is predominantly 6-fold (4-fold)-coordinated in $\text{CaMgSi}_2\text{O}_6$ ($\text{K}_2\text{MgSi}_5\text{O}_{12}$) glass. On the other hand, as expected, the average C_Q for the ^{25}Mg MAS NMR line shape increases by nearly 4 \times in the $\text{CaMgSi}_2\text{O}_6$ glass and by 2 \times in the $\text{K}_2\text{MgSi}_5\text{O}_{12}$ glass, with respect to their crystalline counterparts (Tables 1 and 2), which can be attributed to a corresponding increase in the structural disorder of the Mg coordination environment. Finally, a strong similarity between the ^{25}Mg NMR parameters of $\text{K}_2\text{MgSi}_5\text{O}_{12}$ and $\text{Na}_2\text{MgSi}_3\text{O}_8$ glass indicates a corresponding similarity in their Mg coordination environments (Table 2). These ^{25}Mg MAS NMR results and the general conclusions obtained at the ultrahigh magnetic field of 35.2 T are completely consistent with those obtained in previous studies carried out at 14.1 T, and besides validating each other they do not provide any new information.^{10,13} However, as discussed below, a significantly different structural scenario emerges when the results of the ultrahigh-field ^{25}Mg 3QMAS NMR spectra of these glasses are considered.

The ^{25}Mg 3QMAS NMR spectra of the $\text{CaMgSi}_2\text{O}_6$, $\text{K}_2\text{MgSi}_5\text{O}_{12}$, and $\text{Na}_2\text{MgSi}_3\text{O}_8$ glasses are shown in Figure 3. The total projection of these spectra along the isotropic dimension resolves the presence of at least two Mg resonances in all three cases. For a spin $I = 5/2$ nuclide such as ^{25}Mg , the δ_{iso} and the quadrupolar product $P_Q = C_Q(1 + \eta^2/3)$ for the two resonances can be estimated from their isotropic peak position δ_{F_1} and their center of gravity $\delta_{F_2}^{\text{CG}}$ along the MAS dimension using the following relations²³

$$\delta_{\text{iso}} = \frac{17}{27}\delta_{F_1} + \frac{10}{27}\delta_{F_2}^{\text{CG}} \quad (1)$$

$$P_Q = [(\delta_{F_1} - \delta_{F_2}^{\text{CG}})^{1/2}] \left(\frac{\nu_0}{1000} \right) \sqrt{\frac{680[2I(2I-1)]^2}{81[4I(I+1)-3]}} \quad (2)$$

where ν_0 is the resonance frequency (91.83 MHz) and $I = 5/2$ is the spin quantum number of the nuclide. Such calculations yield δ_{iso} and P_Q values ranging between 12 and 19 ppm and 3.3 and 5.5 MHz, respectively, for one and 30 and 40 ppm and 5.0 and 7.0 MHz, respectively, for the other ^{25}Mg NMR resonance (Table 3). Unfortunately, the structural assignment of these ^{25}Mg resonances on the basis of their δ_{iso} values is not an entirely straightforward task due to the fact that high-resolution ^{25}Mg NMR measurements on well-characterized

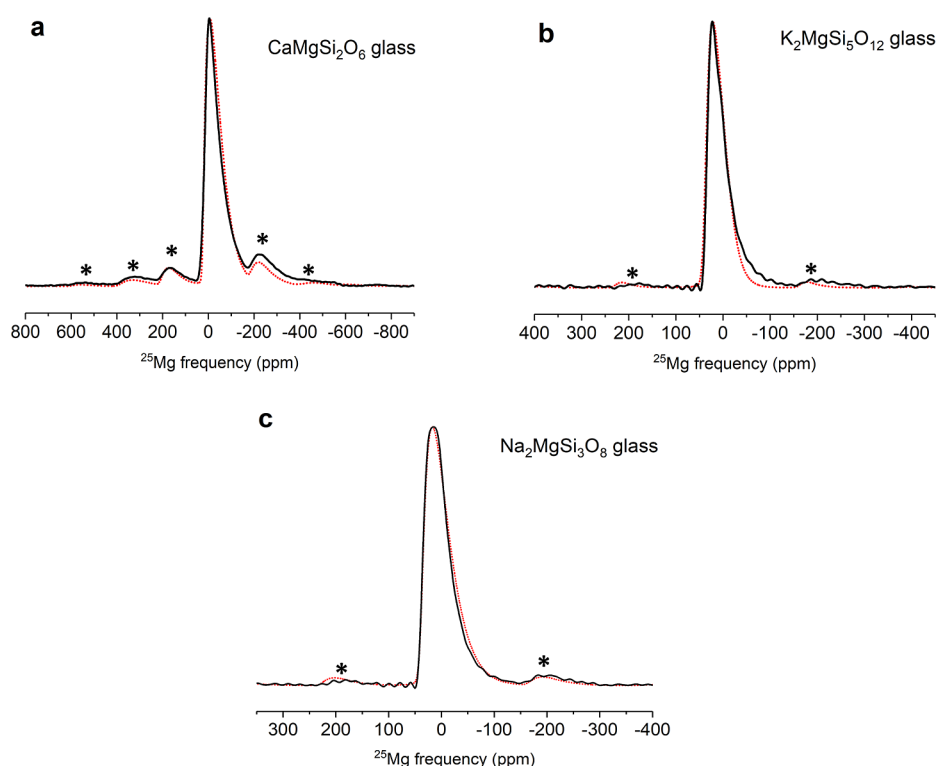


Figure 2. Experimental (solid black line) and simulated (dotted red line) ultrahigh-field (35.2 T) ^{25}Mg MAS NMR spectra of glassy silicates: (a) $\text{CaMgSi}_2\text{O}_6$, (b) $\text{K}_2\text{MgSi}_5\text{O}_{12}$, and (c) $\text{Na}_2\text{MgSi}_3\text{O}_8$. Asterisks denote spinning sidebands. Simulation parameters are listed in Table 2. Note different ppm scales for the spectra.

Table 2. ^{25}Mg NMR Parameters for Glasses Obtained from Simulation of Spectra Acquired at 35.2 T Using a Single Site with an Extended Cjzek Distribution^a

composition	δ_{iso} (± 2 ppm)	average C_Q ^b (± 0.1 MHz)	width of Cjzek distribution σ (± 0.1 MHz)	average η ^b
$\text{CaMgSi}_2\text{O}_6$	16	7.8	2.6	0.0
$\text{K}_2\text{MgSi}_5\text{O}_{12}$	38	6.3	1.2	0.0
$\text{Na}_2\text{MgSi}_3\text{O}_8$	36	6.3	2.0	0.0

^aA Gaussian line-broadening of 10 ppm was used to account for a distribution of isotropic chemical shifts. The mean value of η for the distribution was kept constant for all simulations. ^bMean value of the extended Cjzek distribution.

crystalline compounds remain rather limited in the literature to establish clear chemical shift ranges for specific Mg–O coordination environments in silicates. Previous ^{25}Mg NMR studies^{11,24,25} indicated that the δ_{iso} for Mg^{VI} environments in some silicate minerals ranged between ~ 1 and 15 ppm, while the results of the present study on crystalline silicates as listed in Table 1 indicate that the δ_{iso} for Mg^{IV} environments can at least be as low as ~ 39 ppm. Therefore, the two resonances with low (12–19 ppm) and high (30–40 ppm) δ_{iso} values in the ^{25}Mg 3QMAS NMR spectra of $\text{CaMgSi}_2\text{O}_6$, $\text{K}_2\text{MgSi}_5\text{O}_{12}$, and $\text{Na}_2\text{MgSi}_3\text{O}_8$ glasses can be tentatively assigned to the Mg^{VI} and Mg^{IV} environments, respectively. However, the validity of this assignment hinges somewhat upon whether a fraction of Mg atoms in the structure of these glasses can also be present in 5-fold coordination with oxygen, i.e., as Mg^{V} . Unfortunately, the characteristic δ_{iso} for Mg^{V} species remains unknown at present, though it is expected to lie between ~ 20 and 30 ppm (see below). Nevertheless, the existence of Mg^{V}

species in these glasses cannot be precluded solely on the basis of the NMR data presented in this study.

It may be noted here that in the absence of any constraint on η , the P_Q values obtained from the peak positions in the 3QMAS spectra bracket the estimate of C_Q to within $\pm 15\%$. A second estimate of δ_{iso} and C_Q for these two resonances can be obtained from simulations of the MAS projections of these 3QMAS spectra at the two isotropic peak positions using a Cjzek distribution. These simulations are shown in Figure 4, which yield average δ_{iso} and C_Q values for the Mg^{VI} and Mg^{IV} environments in these glasses that are consistent with the estimates obtained from the 3QMAS spectral peak positions. To ensure further consistency, these average δ_{iso} and C_Q values for the three glasses are used as initial guesses along with an extended Cjzek distribution of the quadrupolar parameters to simulate their 1D ^{25}Mg MAS NMR line shapes in Figure 2. It is clear from Figure 5 that such two-component simulations are indeed able to reproduce the 1D MAS NMR line shapes quite well. The peak areas obtained from these simulations provide the relative fraction of the Mg^{VI} and Mg^{IV} environments in these glasses (Table 3). This procedure yields a $\text{Mg}^{\text{VI}}/\text{Mg}^{\text{IV}}$ ratio of 56:44 for the $\text{CaMgSi}_2\text{O}_6$ glass. This ratio decreases significantly to 30:70 for the $\text{K}_2\text{MgSi}_5\text{O}_{12}$ glass and 25:75 for the $\text{Na}_2\text{MgSi}_3\text{O}_8$ glass. These ratios are found to be completely consistent with those estimated from a simulation of the total isotropic projection spectra with Gaussian components under the assumption of uniform triple-quantum excitation for both Mg environments.

The resulting average Mg–O coordination number of ~ 5.1 for the $\text{CaMgSi}_2\text{O}_6$ glass is consistent with that (~ 5.0) reported on this composition by Ildefonse et al.⁸ on the basis of a Mg K-edge extended X-ray absorption fine structure (EXAFS) spectroscopic study. Moreover, the simulation

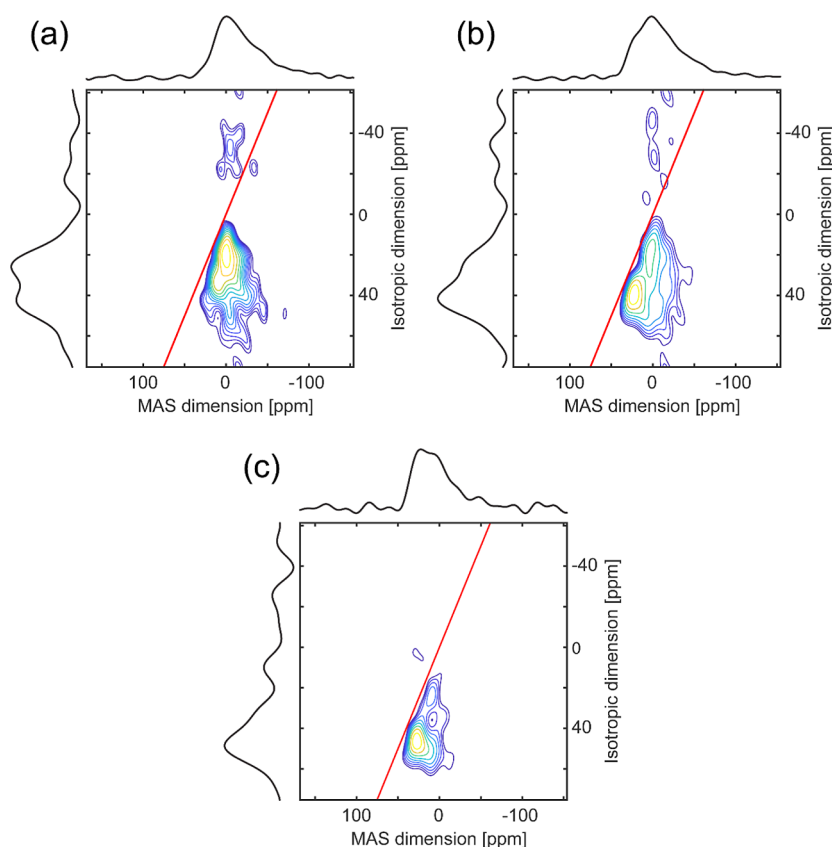


Figure 3. Contour plots of ^{25}Mg 3QMAS NMR spectra of (a) $\text{CaMgSi}_2\text{O}_6$, (b) $\text{K}_2\text{MgSi}_5\text{O}_{12}$, and (c) $\text{Na}_2\text{MgSi}_3\text{O}_8$ glasses. Total projections on isotropic and MAS dimensions are shown on the left and top. The red straight line across each plot denotes a quadrupolar-induced shift.

Table 3. ^{25}Mg NMR Parameters for Glasses Obtained from Simulation of 1D ^{25}Mg MAS Spectra Acquired at 35.2 T Using Two Sites with Extended Czjzek Distributions^a

composition	sites	δ_{iso} (± 2 ppm)	average C_Q (± 0.1 MHz) ^b	width of Czjzek distribution σ (± 0.1 MHz)	average η ^b	relative fraction (%)
$\text{CaMgSi}_2\text{O}_6$	Mg^{IV}	30 (30)	7.7 (7.0)	3.0	0.0	44
	Mg^{VI}	16 (12)	6.0 (5.0)	3.0	0.0	56
$\text{K}_2\text{MgSi}_5\text{O}_{12}$	Mg^{IV}	39 (34)	5.5 (6.0)	0.8	0.0	70
	Mg^{VI}	12 (15)	6.0 (5.5)	2.5	0.0	30
$\text{Na}_2\text{MgSi}_3\text{O}_8$	Mg^{IV}	38 (40)	5.1 (5.0)	2.0	0.0	75
	Mg^{VI}	16 (19)	4.0 (3.3)	3.0	0.0	25

^aA Gaussian line-broadening of 10 ppm was used to account for a distribution of isotropic chemical shifts. The mean value of η for the distribution was kept constant for all simulations. Values in parentheses are δ_{iso} and P_Q obtained from peak positions in F1 and center of gravity positions in F2 dimensions of the 3QMAS spectra using eqs 1 and 2. ^bMean value of the extended Czjzek distribution.

parameters in Table 3 yield an average ^{25}Mg δ_{iso} of ~ 22 ppm, in excellent agreement with the same value reported by George and Stebbins²⁶ for the $\text{CaMgSi}_2\text{O}_6$ liquid using high-temperature ^{25}Mg NMR spectroscopy, lending further support to the Mg–O coordination number obtained in the present study. This Mg–O coordination number is also consistent with that (~ 5.0) obtained in a recent study by Cormier and Cuello²⁷ for glass of composition $\text{Ca}_{1.5}\text{Mg}_{0.5}\text{Si}_2\text{O}_6$ using combined X-ray and neutron diffraction and reverse Monte Carlo simulation. When taken together, this agreement between NMR, EXAFS, and diffraction studies resolves the long-standing inconsistency between the Mg–O coordination numbers for silicate glasses reported in previous studies and the related controversy in the literature, as noted earlier. It is expected that a similar situation will also hold for the MgSiO_3 glass as diffraction studies have indicated that the average Mg–O coordination number for this glass is lower (~ 4.5) compared to its Ca-rich analogues, and

this coordination number monotonically decreases with increasing Mg/Ca in glasses along the binary join CaSiO_3 – MgSiO_3 .^{14,15,27,28}

In a previous study, Kroeker and Stebbins hypothesized that Mg competes more effectively with the low field strength alkali cations than with the higher field strength Ca for the NBOs in the silicate network to form more compact tetrahedral coordination environments. This hypothesis is corroborated by the ^{25}Mg 3QMAS results, which clearly show that compared to the $\text{CaMgSi}_2\text{O}_6$ glass, the $\text{Mg}^{\text{VI}}/\text{Mg}^{\text{IV}}$ ratio is significantly lowered in the alkali–Mg silicate glasses (Table 3). It may be noted that a lowering of the average Mg–O coordination number with increasing Na/Mg ratio was also reported in a previous study by Bisbrouck et al.²⁹ for Na–Mg boroaluminosilicate glasses and a predominantly tetrahedral Mg–O coordination was suggested by Shimoda et al. for Na–Mg and K–Mg silicate glass.¹¹ The results of the present study indicate

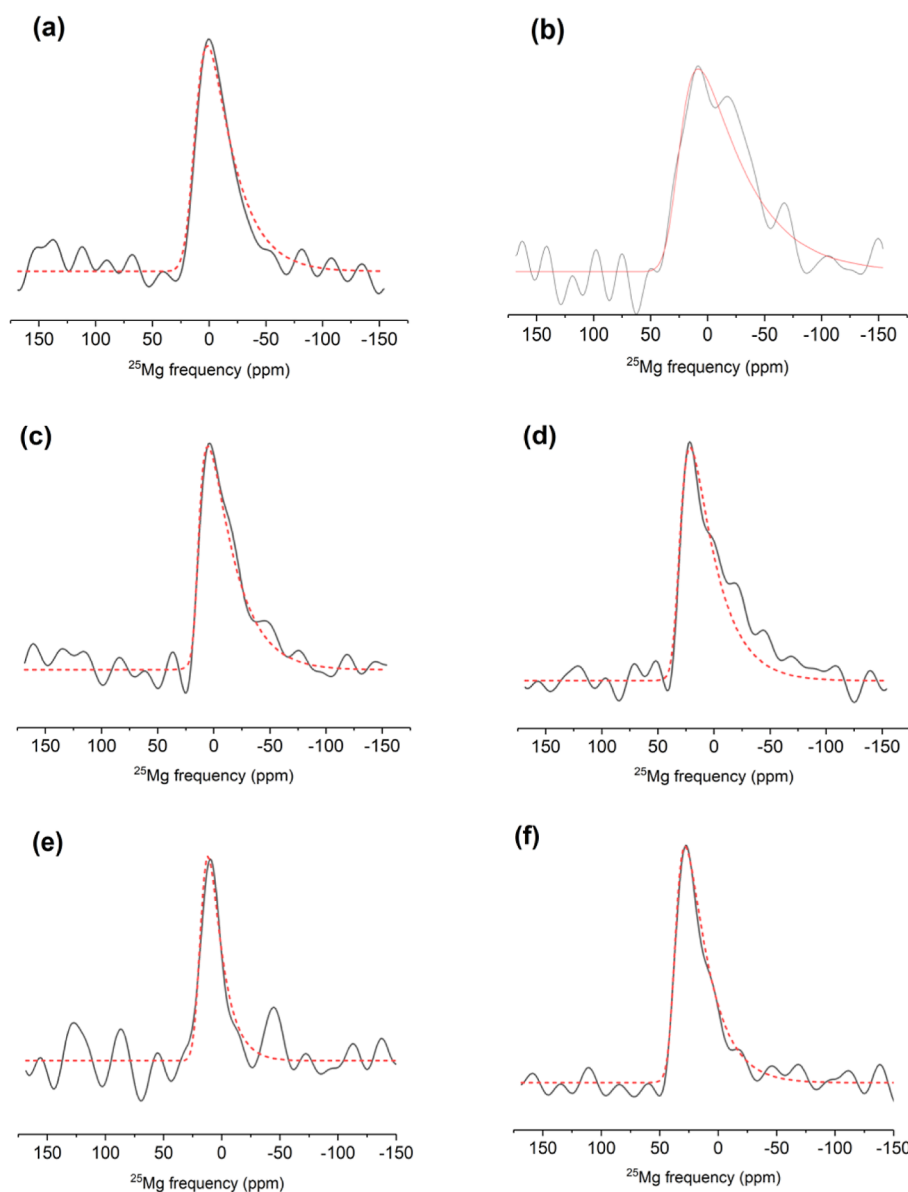


Figure 4. MAS slices of ^{25}Mg 3QMAS spectra at the two isotropic peak positions (solid lines) and corresponding simulations (dashed lines) for $\text{CaMgSi}_2\text{O}_6$, $\text{K}_2\text{MgSi}_5\text{O}_{12}$, and $\text{Na}_2\text{MgSi}_3\text{O}_8$ glasses. MAS slices are taken at isotropic peak positions of (a) 14 and (b) 38 ppm for $\text{CaMgSi}_2\text{O}_6$ glass; (c) 20 and (d) 40 ppm for $\text{K}_2\text{MgSi}_5\text{O}_{12}$ glass; and (e) 25 and (f) 47 ppm for $\text{Na}_2\text{MgSi}_3\text{O}_8$ glass.

that the average Mg–O coordination number is ~ 4.6 for the $\text{K}_2\text{MgSi}_5\text{O}_{12}$ glass and ~ 4.5 for the $\text{Na}_2\text{MgSi}_3\text{O}_8$ glass (Table 3). The average ^{25}Mg δ_{iso} of ~ 31 – 32 ppm for these glasses (Table 3) is again in good agreement with those (~ 27 – 30 ppm) reported by George and Stebbins²⁶ for Na–Mg and Na, K–Mg silicate liquids using high-temperature ^{25}Mg NMR spectroscopy. It may be noted here that the tetrahedral coordination of Mg does not necessarily mean that a part of the Mg ions play the role of network-forming cations in these glasses. This is particularly evident in the ^{29}Si and ^{17}O NMR spectra of glasses of similar compositions reported in the literature, which indicate that the degree of Si–O network connectivity remains consistent with Mg acting as a network modifier in these glasses.^{30–32}

4. CONCLUSIONS

In summary, a combination of ^{25}Mg MAS and 3QMAS NMR at an ultrahigh magnetic field enables identification of mixed

Mg–O coordination environments in silicate glass. The results are interpreted in terms of the coexistence of Mg^{IV} and Mg^{VI} environments in all glasses, although the possibility of the presence of some fraction of Mg in a Mg^{V} environment cannot be ruled out. The relative ratios of Mg^{IV} and Mg^{VI} , thus obtained for $\text{CaMgSi}_2\text{O}_6$ glass, yield an average Mg–O coordination number of ~ 5 , which is in good agreement with the results obtained in previous Mg K-edge EXAFS and diffraction measurements. This agreement resolves a long-standing inconsistency between Mg–O coordination numbers in silicate glasses derived via NMR spectroscopy vis-à-vis X-ray absorption spectroscopy and diffraction techniques. When taken together, the ^{25}Mg δ_{iso} values for various silicate crystals, glasses, and liquids obtained in this study and in previous studies in the literature allow for the establishment of ^{25}Mg chemical shift ranges of ~ 5 – 17 , 20 – 30 , and 30 – 50 ppm, for Mg^{IV} , Mg^{V} , and Mg^{VI} environments, respectively. Mg shows a stronger preference for tetrahedral coordination in alkali–Mg

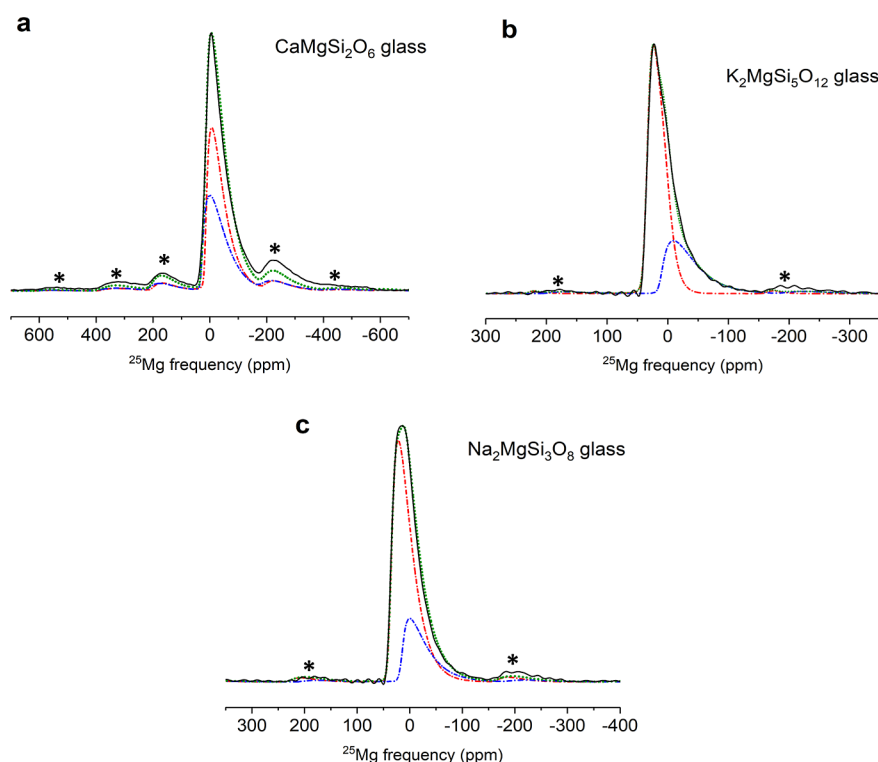


Figure 5. Two-component simulation of experimental 1D ^{25}Mg MAS NMR line shapes (black solid line) for (a) $\text{CaMgSi}_2\text{O}_6$, (b) $\text{K}_2\text{MgSi}_5\text{O}_{12}$, and (c) $\text{Na}_2\text{MgSi}_3\text{O}_8$ glasses. Simulation is shown as a green dotted line and individual components are shown with red and blue dot-dashed lines. Asterisks denote spinning sidebands. Note different ppm scales for the spectra.

silicate glasses compared to $\text{CaMgSi}_2\text{O}_6$ glass, implying that Mg competes for NBO more effectively with low field strength alkali ions than with higher field strength Ca ions. The average ^{25}Mg δ_{iso} values for all glasses are found to be in good agreement with those reported for liquids of similar composition in previous high-temperature ^{25}Mg NMR spectroscopic studies.

AUTHOR INFORMATION

Corresponding Author

Sabyasachi Sen – Department of Materials Science and Engineering, University of California at Davis, Davis, California 95616, United States; orcid.org/0000-0002-4504-3632; Email: sbsen@ucdavis.edu

Authors

Jonathan F. Stebbins – Department of Earth and Planetary Sciences, Stanford University, Stanford, California 94305, United States

Scott Kroeker – Department of Chemistry and Manitoba Institute for Materials, University of Manitoba, Winnipeg, Manitoba R3T 2N2, Canada; orcid.org/0000-0003-1986-2797

Ivan Hung – National High Magnetic Field Laboratory, Tallahassee, Florida 32310, United States; orcid.org/0000-0001-8916-739X

Zhehong Gan – National High Magnetic Field Laboratory, Tallahassee, Florida 32310, United States; orcid.org/0000-0002-9855-5113

Complete contact information is available at: <https://pubs.acs.org/10.1021/acs.jpcb.3c06419>

Notes

The authors declare no competing financial interest.

ACKNOWLEDGMENTS

This work was supported by the Blacutt-Underwood professorship endowment grant to SS. The NHMFL is supported by the National Science Foundation through NSF/DMR-2128556 and the State of Florida. The Development of the 36 T SCH magnet and NMR instrumentation was supported by NSF (DMR-1039938 and DMR-0603042) and NIH GM122698.

REFERENCES

- (1) Bradtmüller, H.; Uesbeck, T.; Eckert, H.; Murata, T.; Nakane, S.; Yamazaki, H. Structural Origins of Crack Resistance on Magnesium Aluminoborosilicate Glasses Studied by Solid-State NMR. *J. Phys. Chem. C* **2019**, *123*, 14941–14954.
- (2) Watts, S. J.; Hill, R. G.; O'donnell, M. D.; Law, R. V. Influence of Magnesia on the Structure and Properties of Bioactive Glasses. *J. Non-Cryst. Solids* **2010**, *356*, 517–524.
- (3) Hu, Y.; Teng, F. Z.; Zhang, H. F.; Xiao, Y.; Su, B. X. Metasomatism-Induced Mantle Magnesium Isotopic Heterogeneity: Evidence from Pyroxenites. *Geochim. Cosmochim. Acta* **2016**, *185*, 88–111.
- (4) Elardo, S. M.; Draper, D. S.; Shearer, C. K., Jr. Lunar Magma Ocean Crystallization Revisited: Bulk Composition, Early Cumulate Mineralogy, and the Source Regions of the Highlands Mg-Suite. *Geochim. Cosmochim. Acta* **2011**, *75*, 3024–3045.
- (5) Rubin, K. H.; Sinton, J. M.; MacLennan, J.; Hellebrand, E. Magmatic Filtering of Mantle Compositions at Mid-Ocean-Ridge Volcanoes. *Nat. Geosci.* **2009**, *2*, 321–328.
- (6) Sen, S.; Maekawa, H.; Papatheodorou, G. N. Short-Range Structure of Invert Glasses Along The Pseudo-Binary Join $\text{MgSiO}_3\text{--Mg}_2\text{SiO}_4$: Results From ^{29}Si and ^{25}Mg MAS NMR Spectroscopy. *J. Phys. Chem. B* **2009**, *113*, 15243–15248.

- (7) Wilding, M. C.; Benmore, C. J.; Tangeman, J. A.; Sampath, S. Coordination Changes in Magnesium Silicate Glasses. *Europhys. Lett.* **2004**, *67*, 212–218.
- (8) Ildefonse, P.; Calas, G.; Flank, A. M.; Lagarde, P. Low Z Elements (Mg, Al, And Si) K-Edge X-Ray Absorption Spectroscopy in Minerals and Disordered Systems. *Nucl. Instrum. Methods Phys. Res., Sect. B* **1995**, *97*, 172–175.
- (9) Dien, L.; Mingsheng, P.; Murata, T. Coordination and Local Structure of Magnesium in Silicate Minerals and Glasses; Mg K-Edge XANES Study. *Can. Mineral.* **1999**, *37*, 199–206.
- (10) Kroeker, S.; Stebbins, J. F. Magnesium Coordination Environments in Glasses and Minerals: New Insight From High-Field Magnesium-25 MAS NMR. *Am. Mineral.* **2000**, *85*, 1459–1464.
- (11) Shimoda, K.; Nemoto, T.; Saito, K. Local Structure of Magnesium in Silicate Glasses: A 25Mg 3QMAS NMR Study. *J. Phys. Chem. B* **2008**, *112*, 6747–6752.
- (12) Shimoda, K.; Tobu, Y.; Hatakeyama, M.; Nemoto, T.; Saito, K. Structural Investigation of Mg Local Environments in Silicate Glasses by Ultra-High Field 25Mg 3QMAS NMR Spectroscopy. *Am. Mineral.* **2007**, *92*, 695–698.
- (13) de Oliveira, M., Jr; Damasceno, H.; Salmon, P. S.; Eckert, H. Analysis and Information Content of Quadrupolar NMR in Glasses: 25Mg NMR in Vitreous MgSiO₃ and CaMgSi₂O₆. *J. Magn. Reson. Open* **2022**, *12*–13, 100067.
- (14) Cormier, L.; Cuello, G. J. Mg Coordination in A MgSiO₃ Glass Using Neutron Diffraction Coupled with Isotopic Substitution. *Phys. Rev. B: Condens. Matter Mater. Phys.* **2011**, *83*, 224204.
- (15) Wilding, M. C.; Benmore, C. J.; Tangeman, J. A.; Sampath, S. Evidence of Different Structures In Magnesium Silicate Liquids: Coordination Changes In Forsterite-To Enstatite-Composition Glasses. *Chem. Geol.* **2004**, *213*, 281–291.
- (16) Frydman, L.; Harwood, J. S. Isotropic Spectra of Half-Integer Quadrupolar Spins From Bidimensional Magic-Angle Spinning NMR. *J. Am. Chem. Soc.* **1995**, *117*, 5367–5368.
- (17) Gan, Z.; Hung, I.; Wang, X.; Paulino, J.; Wu, G.; Litvak, I. M.; Gor'kov, P. L.; Brey, W. W.; Lendi, P.; Schiano, J. L.; et al. NMR Spectroscopy Up To 35.2 T Using A Series-Connected Hybrid Magnet. *J. Magn. Reson.* **2017**, *284*, 125–136.
- (18) Larsen, F. H.; Jakobsen, H. J.; Ellis, P. D.; Nielsen, N. C. Sensitivity-Enhanced Quadrupolar-Echo NMR of Half-Integer Quadrupolar Nuclei. Magnitudes and Relative Orientation of Chemical Shielding and Quadrupolar Coupling Tensors. *J. Phys. Chem. A* **1997**, *101*, 8597–8606.
- (19) Brown, S. P.; Wimperis, S. Two-Dimensional Multiple-Quantum MAS NMR of Quadrupolar Nuclei: A Comparison of Methods. *J. Magn. Reson.* **1997**, *128*, 42–61.
- (20) Harris, R. K.; Becker, E. D.; Cabral de Menezes, S. M.; Goodfellow, R.; Granger, P. NMR Nomenclature: Nuclear Spin Properties and Conventions for Chemical Shifts. IUPAC Recommendations 2001. International Union of Pure and Applied Chemistry. Physical Chemistry Division. Commission on Molecular Structure and Spectroscopy. *Magn. Reson. Chem.* **2002**, *40*, 489–505.
- (21) Van Meerten, S. G. J.; Franssen, W. M. J.; Kentgens, A. P. ssNake: A cross-platform open-source NMR data processing and fitting application. *J. Magn. Reson.* **2019**, *301*, 56–66.
- (22) d'Espinose de Lacaillerie, J. B.; Fretigny, C.; Massiot, D. MAS NMR Spectra of Quadrupolar Nuclei in Disordered Solids: The Czjzek Model. *J. Magn. Reson.* **2008**, *192*, 244–251.
- (23) Amoureux, J. P.; Huguénard, C.; Engelke, F.; Taulelle, F. Unified Representation of MQMAS and STMAS NMR of Half-Integer Quadrupolar Nuclei. *Chem. Phys. Lett.* **2002**, *356*, 497–504.
- (24) MacKenzie, K. J. D.; Meinhold, R. H. 25Mg Nuclear Magnetic Resonance Spectroscopy of Minerals and Related and Inorganics: A Survey Study. *Am. Mineral.* **1994**, *79*, 250–260.
- (25) Pallister, P. J.; Moudrakovski, I. L.; Ripmeester, J. A. Mg-25 Ultra-high Field Solid State NMR Spectroscopy and First Principles Calculations of Magnesium Compounds. *Phys. Chem. Chem. Phys.* **2009**, *11*, 11487–11500.
- (26) George, A. M.; Stebbins, J. F. Structure and Dynamics of Magnesium in Silicate Melts: A High-Temperature 25Mg NMR Study. *Am. Mineral.* **1998**, *83*, 1022–1029.
- (27) Cormier, L.; Cuello, G. J. Structural Investigation Of Glasses Along the MgSiO₃–CaSiO₃ Join: Diffraction Studies. *Geochim. Cosmochim. Acta* **2013**, *122*, 498–510.
- (28) Salmon, P. S.; Moody, G. S.; Ishii, Y.; Pizzey, K. J.; Polidori, A.; Salanne, M.; Zeidler, A.; Buscemi, M.; Fischer, H. E.; Bull, C. L.; Klotz, S.; et al. Pressure Induced Structural Transformations in Amorphous MgSiO₃ and CaSiO₃. *J. Non-Cryst. Solids: X* **2019**, *3*, 100024.
- (29) Bisbrouck, N.; Bertani, M.; Angeli, F.; Charpentier, T.; de Ligny, D.; Delaye, J. M.; Gin, S.; Micoulaut, M. Impact of Magnesium on The Structure of Aluminoborosilicate Glasses: A Solid-State NMR and Raman Spectroscopy Study. *J. Am. Ceram. Soc.* **2021**, *104*, 4518–4536.
- (30) Fiske, P. S.; Stebbins, J. F. The Structural Role of Mg in Silicate Liquids: A High-Temperature ²⁵Mg, ²³Na, and ²⁹Si NMR Study. *Am. Mineral.* **1994**, *79*, 848–861.
- (31) Park, S. Y.; Lee, S. K. Structure and Disorder in Basaltic Glasses And Melts: Insights From High-Resolution Solid-State NMR Study of Glasses in Diopside–Ca-Tschermakite Join and Diopside–Anorthite Eutectic Composition. *Geochim. Cosmochim. Acta* **2012**, *80*, 125–142.
- (32) Allwardt, J. R.; Stebbins, J. F. Ca-Mg and K-Mg mixing around non-bridging O atoms in silicate glasses: An investigation using ¹⁷O MAS and 3QMAS NMR ¹⁷O MAS And 3QMAS NMR. *Am. Mineral.* **2004**, *89*, 777–784.